

DOE/PC/79907--T8

DE91 000634

QUARTERLY REPORT

December 15, 1989 to March 14, 1990

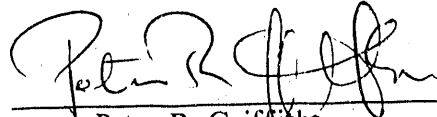
DOE Grant No.: DE-FG22-87PC79907

SPECTROSCOPIC STUDY OF COAL STRUCTURE AND REACTIVITY

Report From: Peter R. Griffiths
Department of Chemistry
University of Idaho
Moscow, ID 83843

Principal Investigator: Dallas L. Rabenstein
Department of Chemistry
University of California, Riverside
Riverside, CA 92521

Project Officer: Dr. Dennis Finseth, MS 94-101
Pittsburgh Energy Technology Center
U.S. Department of Energy
Pittsburgh, PA 15236

Signed: 
Peter R. Griffiths

Date: 9-7-90

MASTER
DISTRIBUTION OF THIS DOCUMENT IS UNLIMITED
ps

Summary

Work done during this period (December 15, 1989 to March 14, 1990) covered two of the three primary areas of study of this project. The first involved the continuing development of a step-scanning interferometer for the photoacoustic depth-profiling of materials whose composition varies in the spatial region between 5 and 50 μm from its surface. The second covered the initial construction of an on-line interface between a supercritical fluid chromatograph (SFC) and a Fourier transform infrared (FT-IR) spectrometer for monitoring the composition of coal extracts.

Step-Scanning Interferometer

The electronic circuit to control the new Inchworm (IW) drive described in the previous Quarterly Report was implemented. The computer contains a digital input/output (I/O) board (Metrabyte PIO-24) that is used to control the drive mechanism. The computer sends commands directly to the IW controller (Burleigh Instruments, Model 6000) in the form of a TTL signal to define the direction of motion and a series of pulses to advance the drive. Each transition (HI-LO and LO-HI) counts as one step. Had the step size of the IW been constant at 4 nm, as we had assumed from the manufacturer's literature, controlling the mirror motion would have been a simple matter, and the moving mirror could have been advanced rapidly from one sampling position to the next. Because of the problems that were described in the previous Quarterly Report, we were forced to use the approach that we had implemented previously with the stepper-motor drive, namely to move the mirror slowly and to monitor the interference record until the appropriate number of laser fringes had been recorded. The speed at which the mirror can be moved using this approach must be quite slow, as the computer has to take the time to measure the voltage from the laser detector and decide whether to continue to stop the motion. Furthermore, it is possible to make an error in counting the fringes properly because of the flaws in the laser interference record caused by the clamping cycle (see previous Quarterly Report). It is, of course, absolutely necessary never to miscount fringes because an error will be introduced into the retardation axis that will completely ruin the resulting spectrum. The present implementation of the step-scanning interferometer deals with this problem by giving up the high speed of travel and measuring the laser interference record more frequently than should be absolutely necessary for counting fringes.

By taking the precautions described above, excellent performance in the mirror drive has been achieved. The typical signal from the PZT control circuit for a 2000-point interferogram is shown in Figure 1. The straight lines at the top and bottom of the plot represent the maximum and minimum values of the laser interference record. The points in the middle of the plot are the readings of the laser signal while the control circuit is engaged in order to maintain the mirror position at the LZC. There are one or two bad (but not unacceptable) points, but overall the reproducibility is excellent. The laser values have been transformed into optical retardation in nanometers. The standard deviation of the position distribution is only 2.2 nm about a mean position of 1.5 nm away from the LZC, see Figure 2.

The computer runs a program (IWscan9) to complete a scan. The program follows these steps. The user inputs the following scan parameters: data filename, number of data points, position of the centerburst in the interferogram, number of reference laser fringes between data points, the settle time, the number of ADC conversions to be averaged for each data point, and the ADC frequency. The program then actuates the mirror movement and records the laser voltage while keeping track of the maximum and minimum values. At some point determined by the user, this process is stopped and the LZC is set at the average of the maximum and minimum values. This value is output to the PZT control. The mirror is then moved to the starting location of the scan and the program waits to initiate the scan. This allows the user to set the lock-in amplifier (LIA) parameters and any other experimental aspects before starting the scan.

When the scan is started, a program loop is initiated that repeats the same procedure for each data point. This procedure consists of a number of steps. The PZT is reset to its mid-point extension (so that the feedback circuit is not running during the motion over the fringes). The IW is moved while monitoring the laser voltage. After the requested number of fringes is passed, the IW is stopped and the PZT is engaged. At this point, the program waits for the settle time. This settle time allows for two things to happen. First, the PZT is given time to reach the LZC position. Second, one needs to wait for the LIA to reach the proper values in the in-phase and quadrature channels. The LIA has a time constant associated with the demodulation and thus the output cannot change instantaneously with a change in the input signal. If one changed from an input of 0 to 1 instantly, one needs to wait about 5 time constants for the output to reach a reasonable approximation

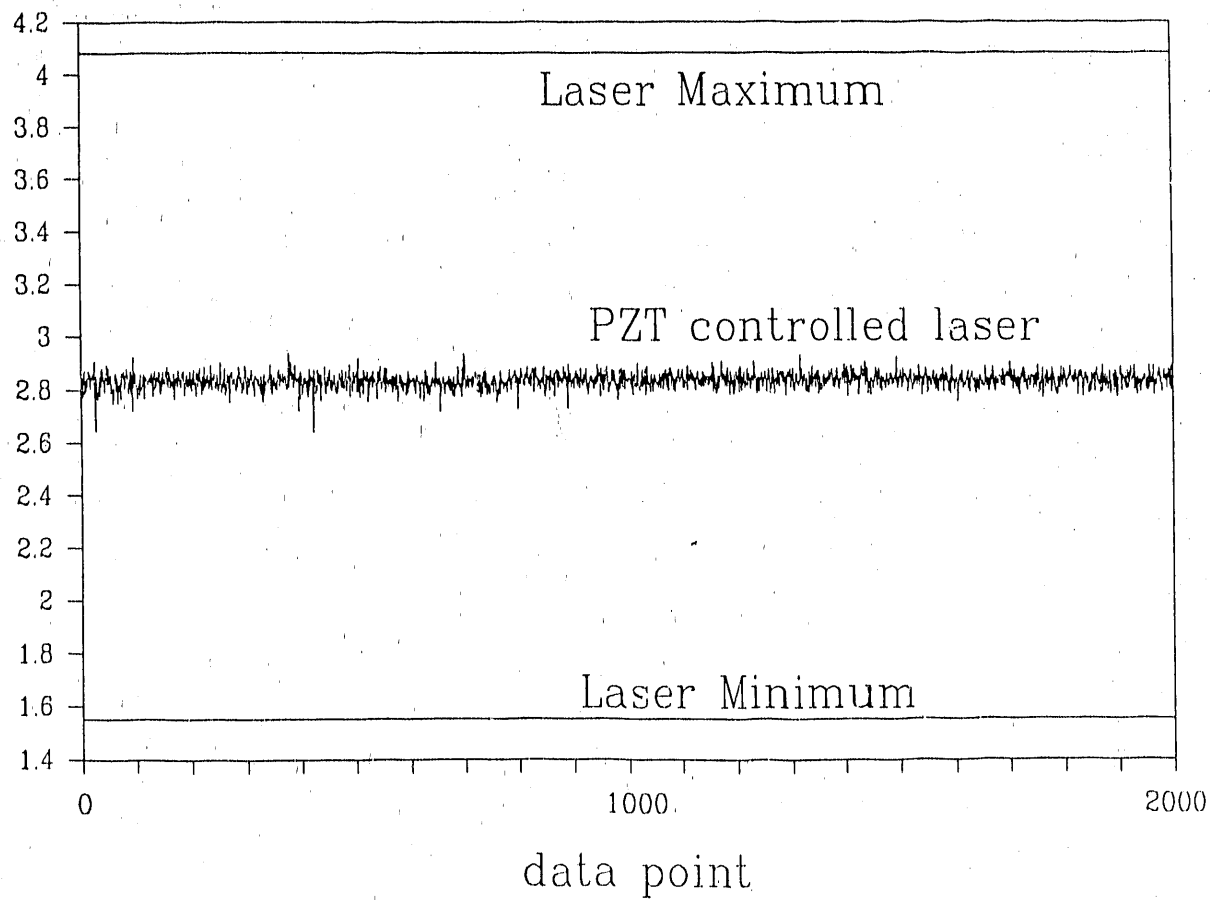


Figure 1. Typical output signal from the PZT control circuit.

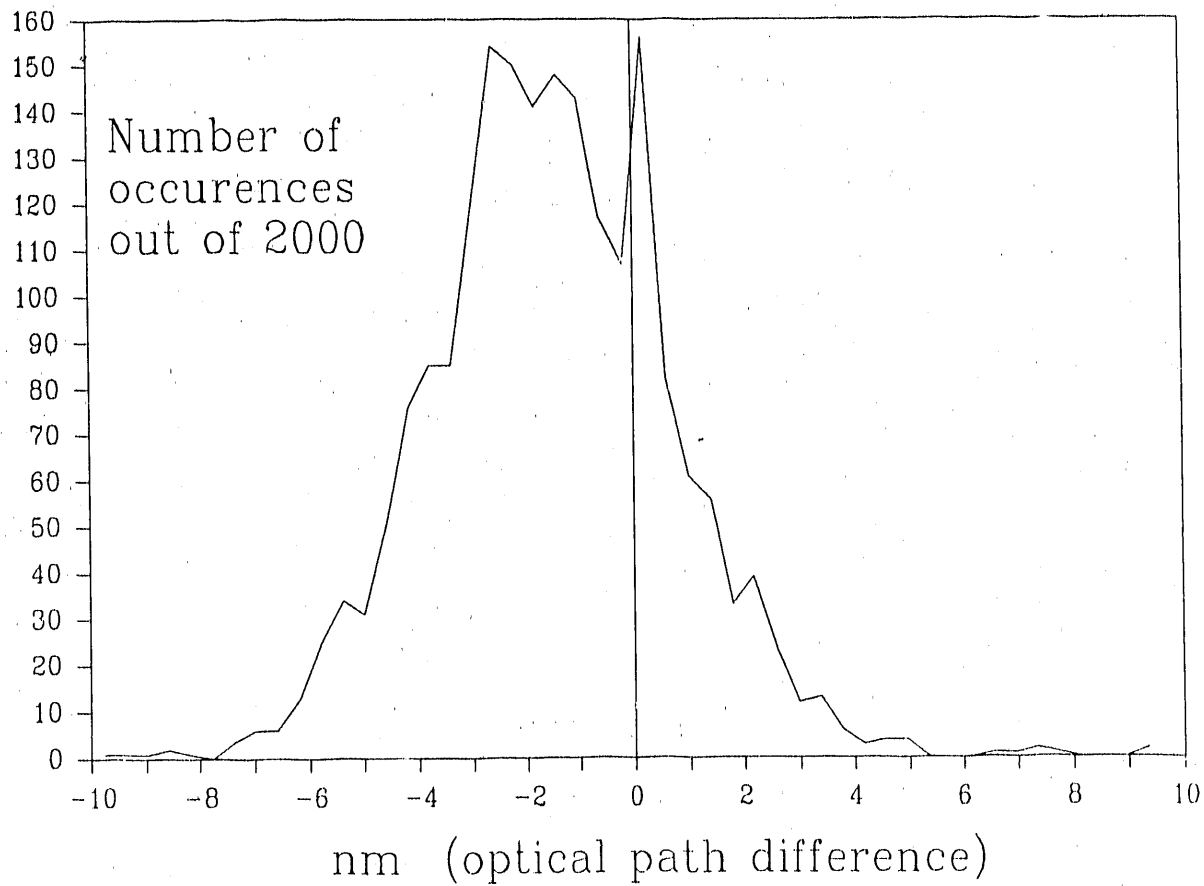


Figure 2. Mirror position error during a 2000-point interferogram.

to 1 (actually 0.995). In most of the experiments done with this system, it is this settle time that accounts for most of the total scan time. Settle times of 2 to 5 seconds are usual, thus a 2048 point scan will take 1 to 3 hours not counting any time for movement or data collection. After the settle time is over the laser value is measured and recorded in an information data file. Then each of the four channels is measured the requested number of times at the requested frequency. The means of these readings are written to four data files (one for each channel). The laser voltage is recorded again and the IW position and the time also recorded to the information data file. The procedure is then repeated.

There are optimal settings for the LIA time constant, settle time and time spent doing A/D conversions depending on the parameter of the experiment and the noise characteristics. The first concern is that the settle time has to be great enough to allow the PZT to get the mirror to the proper position. This depends on the quality of the initial positioning by the inchworm and the speed of the response of the circuit. We have found that 2 seconds are usually needed for this operation. Fortunately, this time also counts towards settling the LIA (unless the first derivative of the signal with respect to mirror position is very high). The time constant on the LIA needs to be fully demodulated. Larger time constants than this minimum will provide signal averaging to reduce the noise but only from those noise sources above the LIA in the signal stream (such as detector noise but not A/D noise). The greater the time spent doing A/D conversions the better as far as signal averaging goes, but one must remember that the signal from the LIA will not vary faster than its time constant. Thus for a time constant of 1 second, for 5 seconds of data collection an A/D converter will measure 5 independent values (signal plus 5 independent draws of the pre-LIA noise) regardless of the ADC frequency. Thus when operating under a constraint of total time spent for a data point (settle time + collection time), there are some optimal values. The minimum possible LIA time constant is the greater of 2 ms or 5 times the modulation period. The settle time is set at 5 times the time constant and the collection time is set at the remaining available time. The shortest possible LIA time constant is desired because, although the LIA time constant and the ADC signal averaging time are equivalent in nature, the LIA time constant counts against you twice, once for the settle time and once for the lack of independent measures in the collection time. Furthermore, the LIA does not integrate out any noise that is introduced between the output of the LIA and the

the LIA does not integrate out any noise that is introduced between the output of the LIA and the ADC.

During this period of the project, another serious form of noise was observed that greatly reduced our productivity. We have designated this noise problem the "bilevel effect" because of its manifestation. Distinct steps (up and down between two levels) in the data occur at random times. The amplitude of the step and the frequency of occurrence within a single scan are variable. Figure 3 shows a typical interferogram measured with a photoacoustic (PA) detector where the bilevel effect is readily visible. Sometimes the amplitude of the effect is so small that it is not visible in the interferogram but is manifested as a degradation in the signal-to-noise ratio (SNR) of the spectrum. The effect can go away for long periods of time then mysteriously reappear. It was not associated with the well-known "five o'clock effect", but it will be described in this Quarterly Report as most of the effort in tracking it down was expended during this period.

Several possible causes were postulated, of which the most likely were believed to be a deficiency with the LIA or a problem with the PA cell or its associated preamplifier. The signal from the PA preamplifier was input to two identical lock-in amplifiers, mounted in parallel. One of these LIAs had just been checked out by the manufacturer and should have been free from defects. Since the bilevel effect was observed in the output from both LIAs, we believed that the results of this experiment showed that the problem could not be associated with this component. We observed the same effect when the PA cell was replaced by a conventional deuterated triglycine sulfate (DTGS) pyroelectric detector, thereby eliminating the PA cell or its amplifier as the cause.

After many weeks, the problem was eventually tracked down to the reference output of the chopper controller. By looking at the actual data collected for one data point (instead of just the average), it was seen that the data flipped between two states, one in which the signal was "good", i.e. it had low variance, and one where it was bad (high variance with a shift). When it was present, the effect seemed to have a regular frequency of about 0.05 Hz (with an additional small 6 Hz component). Another very strange aspect of this effect was that it sometimes only appeared in the quadrature channels of the lock-in amplifiers, regardless of the LIA phase setting.

We are now convinced that the problem must be in the chopper reference signal generator because the effect appears with both PA and DTGS detectors and with two LIAs in a highly

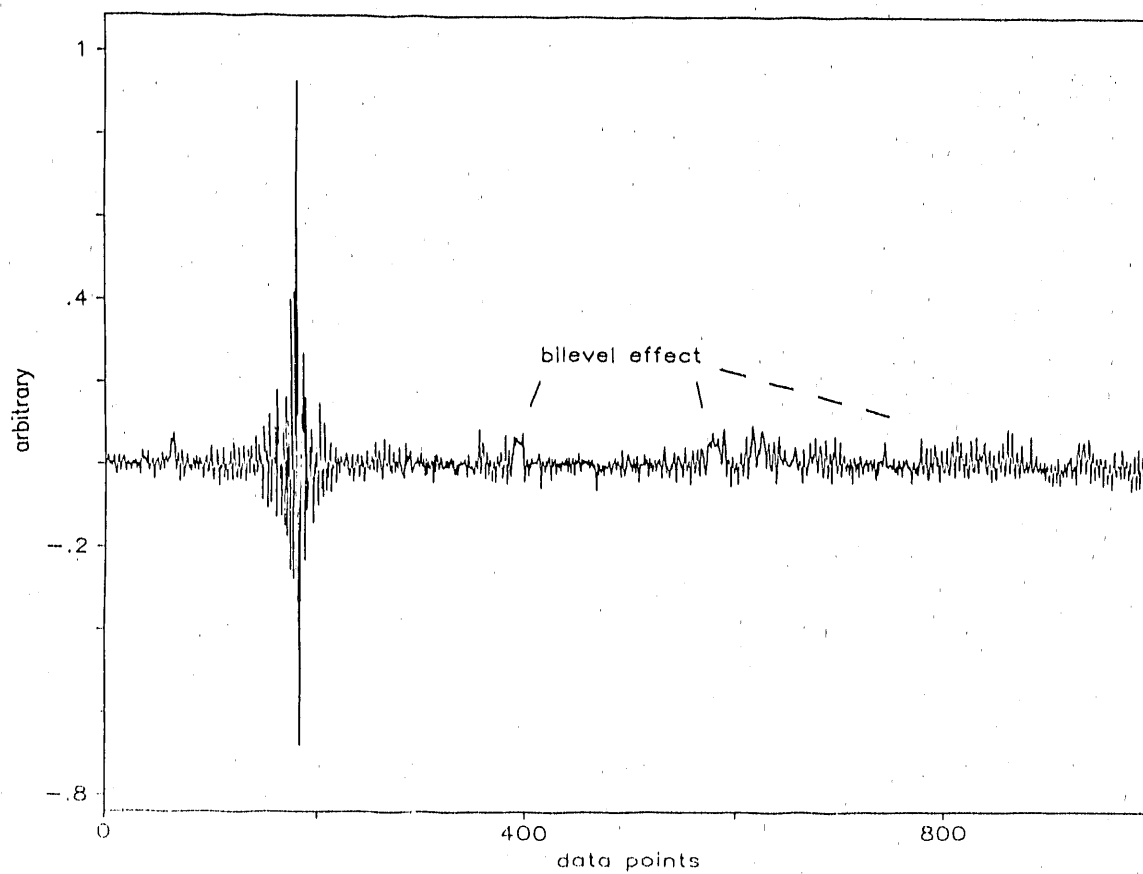


Figure 3. Interferogram illustrating the occurrence of the "bilevel effect".

correlated manner. The only shared component is the chopper and the chopper wheel should not cause any problems because of its inertia. Furthermore, any flaw in the chopper wheel itself should show up in both the in-phase and quadrature channels of the LIA because it would affect the phase of the signal. We are currently fabricating a new circuit to give a better reference to the LIA and hope that this solves the problem.

When the bilevel effect is absent, the step-scanning interferometer yields high quality photoacoustic spectra. The PA interferogram of polyethylene powder (in-phase only) is shown in Figure 4. This interferogram was measured with a modulation frequency of 250 Hz and a LIA time constant of 300 ms. 2000 data points were collected at a spacing of one laser fringe ($0.6328 \mu\text{m}$ retardation) and a 2-s settle time. The LIA phase was set at 156.8° to maximize the in-phase component. The scan took 2 hours and 20 minutes to complete and produced an 8 cm^{-1} resolution spectrum between 0 and 7900 cm^{-1} . As will be seen in future reports, there is a strong need to acquire both the in-phase and quadrature signals from the LIA if photoacoustic depth-profiling is to yield useful and accurate results. The in-phase and quadrature spectra measured from the polyethylene sample whose in-phase interferogram is shown in Figure 4 are shown in Figure 5. The SNR of these spectra indicates that, when the bilevel effect is finally eliminated, the performance of the step-scanning interferometer being constructed in this project will be high enough to permit variations in the composition of samples to be studied at distances of up to 40 or $50 \mu\text{m}$ from their surface.

Development of the SFC/FT-IR Interface

Several years ago, we described techniques whereby both gas chromatography (GC) [1,2] and SFC [3,4] eluents could be trapped as very small (about $100\text{-}\mu\text{m}$ diameter) spots on a ZnSe window. The infrared spectra of the trapped components could be measured using an FT-IR microscope. By reducing the diameter of the deposit, detection limits could be reduced to the subnanogram regime. This technique was applied to the characterization of coal extracts after separation by SFC during the previous year of this project. The Digilab Division of Bio-Rad Laboratories recently introduced a GC/FT-IR interface (the "Tracer") that was based on this principle [5]. During this project period, we have started to modify the Tracer GC/FT-IR interface for on-line SFC/FT-IR measurements.

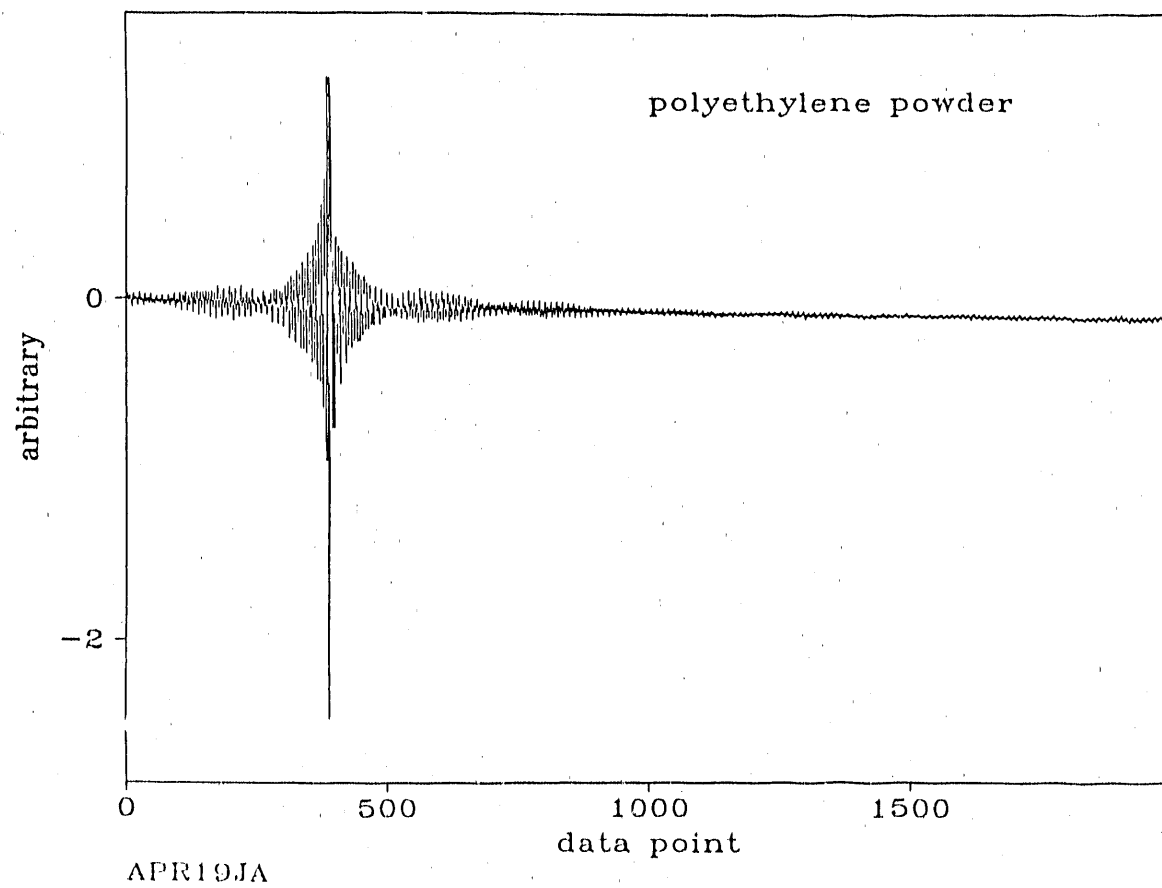


Figure 4. Photoacoustic interferogram of polyethylene powder (in-phase component) measured using a step-scanning interferometer in the absence of the bilevel effect.

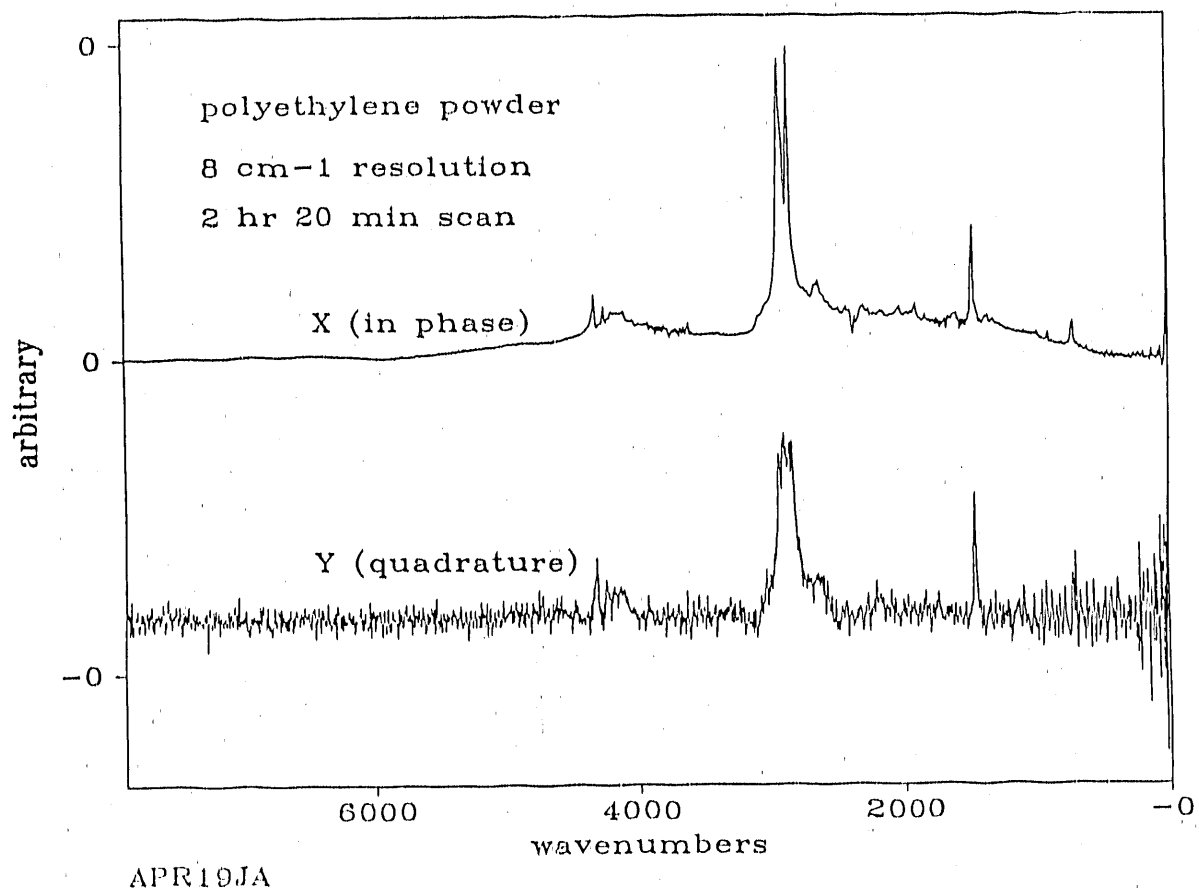


Figure 5. In-phase and quadrature photoacoustic polyethylene powder. The in-phase spectrum is the transform of the interferogram shown in Figure 4.

All previous work on this part of this project had involved the deposition of SFC elutes on a stationary ZnSe window. The window was moved discretely so that each peak was deposited on a different region of the window. In this report, the first on-line direct deposition SFC/FT-IR results obtained in our laboratory (or any other lab in the world) are described.

The performance of the Tracer GC/FT-IR interface is described in a manuscript that has just been accepted for publication by Analytical Chemistry [5]. The Tracer was configured for SFC/FT-IR by mounting a frit restrictor about 100 μm above the moving ZnSe window. The window was held at 0°C so that the elutes from the SFC column would condense and the mobile phase would evaporate away immediately on emerging from the restrictor. A frit restrictor was employed for the initial study. The factors affecting the deposition of SFC elutes were investigated using compounds of fairly high polarity but which previous experience in this laboratory had shown to give relatively narrow peaks. The probe compound that we had used most often in our laboratory was acenaphthenequinone [1,3]. All data obtained this quarter involved the use of just this compound.

The chromatogram of a 60-nL injection of a 0.1% solution of acenaphthenequinone in CH_2Cl_2 after elution from a biphenyl column at 70°C using neat CO_2 measured using a flame ionization detector (FID) is shown in Figure 6. The following pressure program was used:

Initial Pressure: 2000 psi (hold for 5 minutes)
Pressure Ramp: 50 psi/min
Final Pressure: 3500 psi (reached after 22 minutes)

The baseline of this chromatogram is seen to be well above zero, possibly because of the very slow elution of the last traces of the solvent. The full width at half height (FWHH) of the peak in this chromatogram is approximately 30 sec.

The same sample was then measured using the direct deposition SFC/FT-IR interface that had been constructed by modifying the Bio-Rad Tracer GC/FT-IR interface. All data were measured on-line, i.e., as the deposited sample passed through the infrared beam which was 100 μm in diameter. Blocks of 16 scans were measured with the window stationary. The window was then advanced before the next set of 16 scans was measured. The chromatogram was constructed from the measured infrared data both by applying the Gram-Schmidt vector orthogonalization algorithm (see Figure 7, lower trace) and by calculating the integrated absorbance in the region of the C=O

Acenaphthenequinone

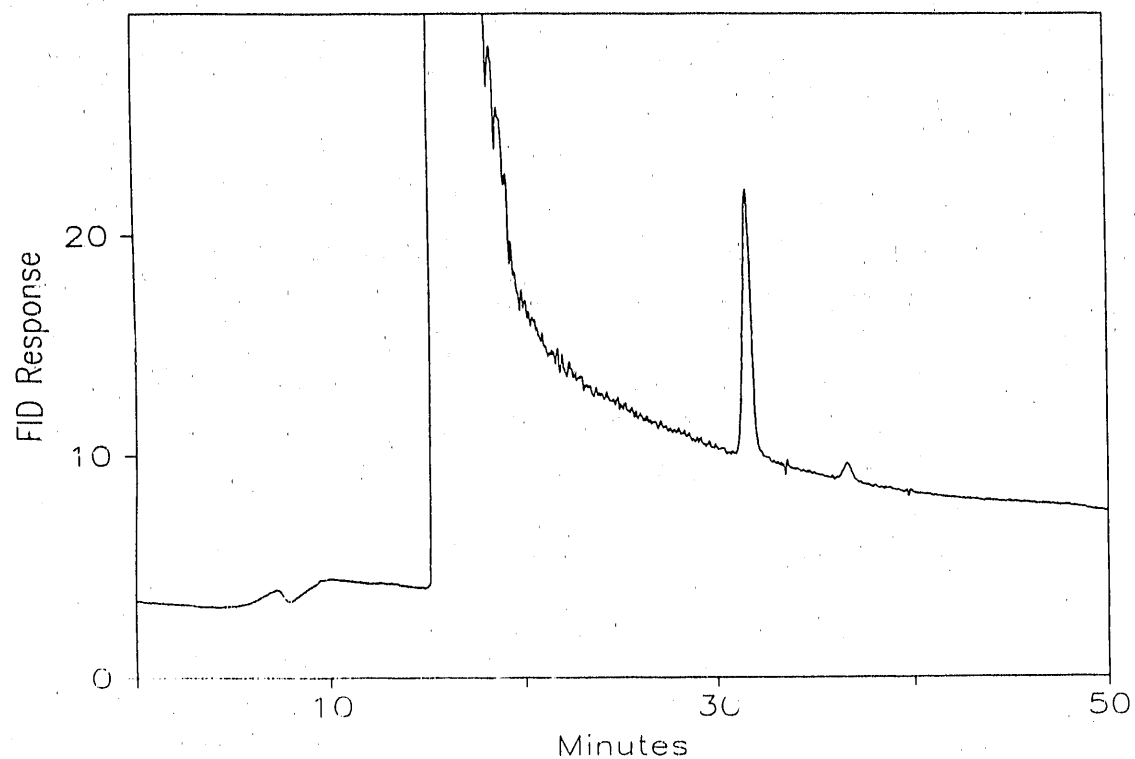


Figure 6. Capillary supercritical fluid chromatogram of 0.1% solution of acenaphthenequinone measured with a flame ionization detector.

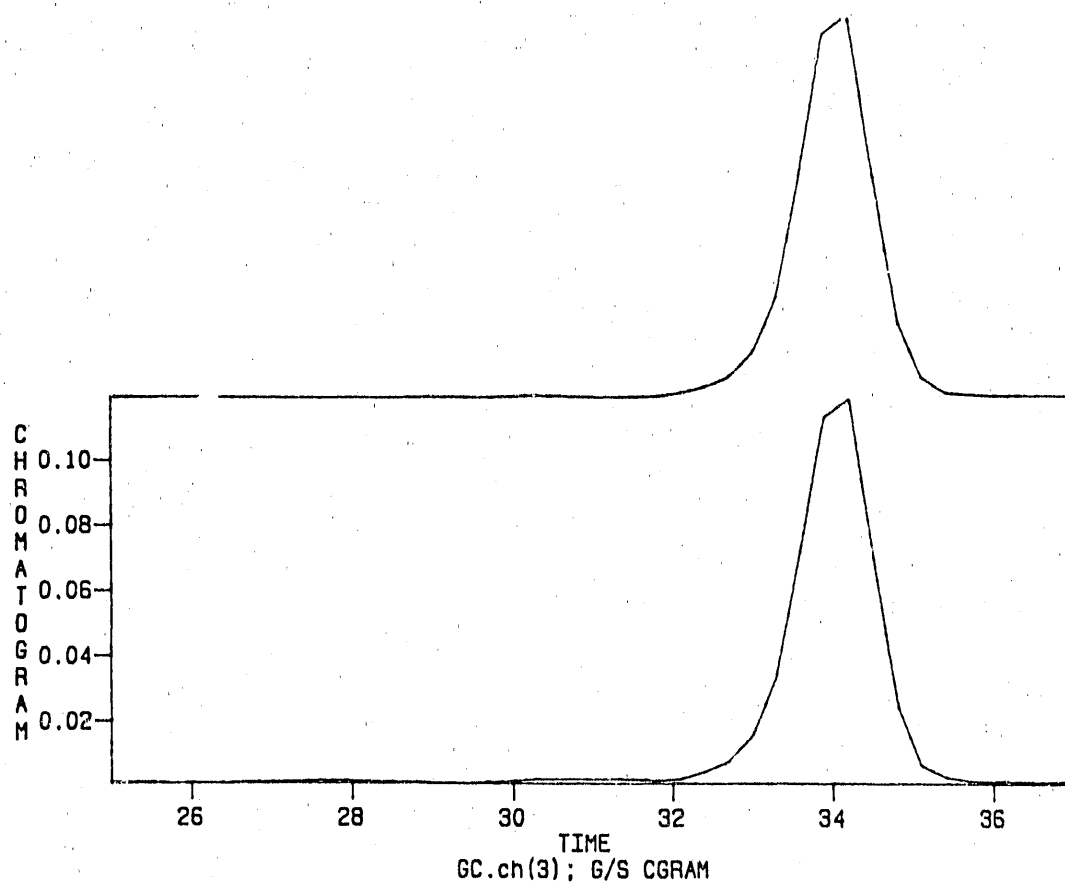


Figure 7. Reconstructed chromatograms of acenaphthenequinone peak measured using (lower trace) Gram-Schmidt and (upper trace) integrated absorbance algorithms.

stretching mode (see Figure 7, upper trace). Both traces were essentially identical, and had a higher signal-to-noise ratio (SNR) than the chromatogram measured with a flame ionization detector. The baseline was at zero, indicating that the material in the column effluent causing the "baseline" to be raised above zero in the FID chromatogram was not present when the interferograms were being measured. The logical explanation for this difference is that the raised baseline in the FID chromatogram was caused by a low level of volatile material eluting throughout the chromatogram; as noted above, this was probably the tail of the very broad solvent peak.

The only problem with the infrared chromatograms was that the FWHH of the peak was approximately 60 seconds, i.e., the FWHH was twice as high as in the FID chromatogram. The thickness profile of the spot of acenaphthenequinone was measured and the diameter of the spot was found to be about 350 μm . This was much greater than had been found in previous studies in our laboratory, where a diameter of between 100 and 150 μm was commonly measured. The previous study had been made using an integral restrictor; thus the difference between the on-line result and the previous off-line data was ascribed to the use of the frit restrictor.

Despite the large diameter of the deposit, the quality of the measured spectrum of acenaphthenequinone was very good. The spectrum of the scan set corresponding to the largest point on the reconstructed chromatogram is shown in Figure 8. Note that this spectrum was measured using an aperture of 100 μm , even though the diameter of the spot of acenaphthenequinone was 350 μm . Had the diameter of the deposit been reduced to 100 μm (which we know to be feasible from our previous work with an integral restrictor), the thickness of the acenaphthenequinone deposit would have been increased by about an order of magnitude, i.e., $(350/100)^2$. In this case, the absorbances of each band in the spectrum (and hence the SNR) would be increased by a factor of ten. How close we come to meeting this goal after installation of an integral restrictor will, hopefully, be reported in the next Quarterly Report.

References

1. R. Fuoco, K.H. Shafer, and P.R. Griffiths, Anal. Chem., **58**, 3249 (1986).
2. A.M. Haefner, K.L. Norton, P.R. Griffiths, S. Bourne, and R. Curbelo, Anal. Chem., **60**, 2441 (1988).

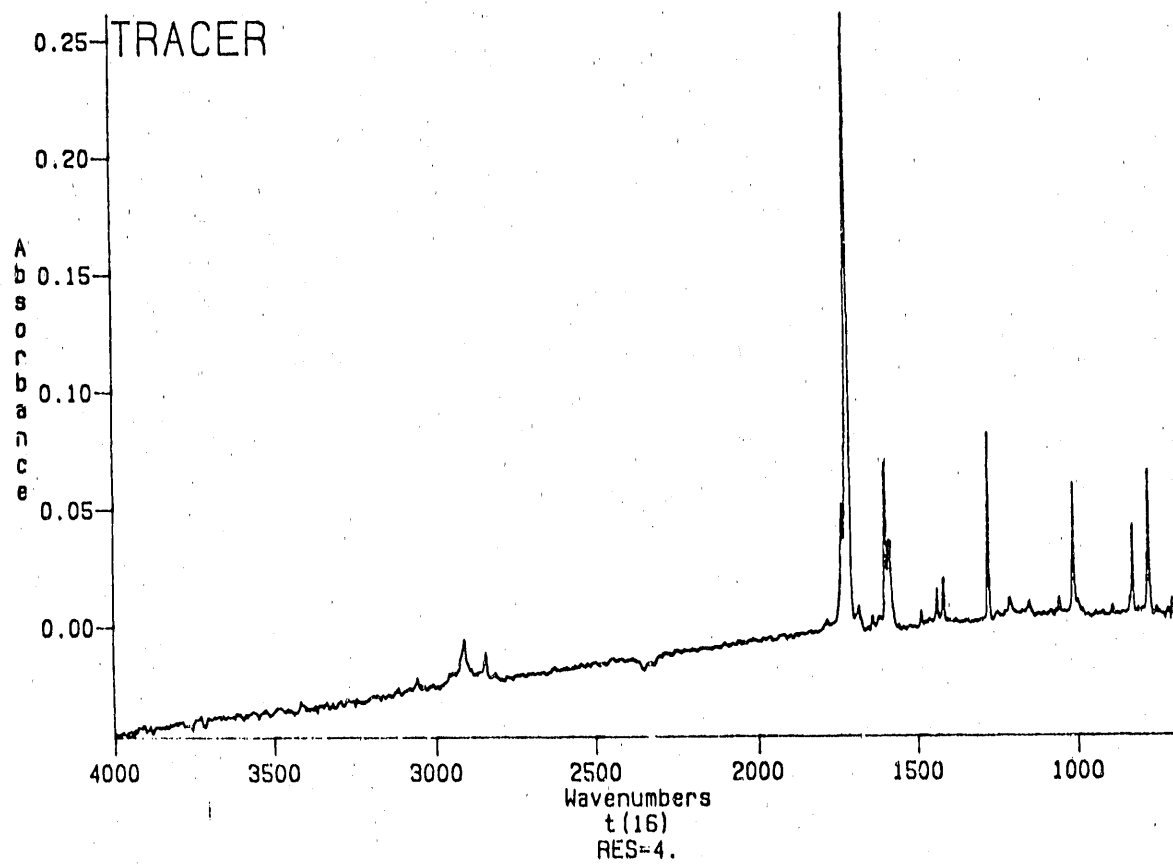


Figure 8. Spectra of 60-ng of acenaphthenequinone calculated from the most intense data point in the chromatograms shown in Figure 7.

3. S.L. Pentoney, K.H. Shafer, P.R. Griffiths, and R. Fuoco, J. High Res. Chromatogr., 9, 168 (1986).
4. S.L. Pentoney, K.H. Shafer and P.R. Griffiths, J. Chromatogr. Sci., 24, 230-235 (1986).
5. S. Bourne, A.M. Haefner, K.L. Norton, and P.R. Griffiths, Anal. Chem., in press (1990).

DISCLAIMER

This report was prepared as an account of work sponsored by an agency of the United States Government. Neither the United States Government nor any agency thereof, nor any of their employees, makes any warranty, express or implied, or assumes any legal liability or responsibility for the accuracy, completeness, or usefulness of any information, apparatus, product, or process disclosed, or represents that its use would not infringe privately owned rights. Reference herein to any specific commercial product, process, or service by trade name, trademark, manufacturer, or otherwise does not necessarily constitute or imply its endorsement, recommendation, or favoring by the United States Government or any agency thereof. The views and opinions of authors expressed herein do not necessarily state or reflect those of the United States Government or any agency thereof.

END

DATE FILMED

10 / 26 / 90

